A Wide Frequency Range CMOS Active Inductor for UWB Bandpass Filters

Md. Mahbub Reja, Kambiz Moez and Igor Filanovsky,
Dept. of ECE, University of Alberta, Edmonton, Alberta, Canada,
Email:mreja@ece.ualberta.ca

Abstract

***Abstract*— A CMOS active inductor that exhibits wide-frequency range inductive impedance with a high quality factor (Q) is presented. The inductor is designed using negative impedance obtained in a cross-coupled transistor pair that is a part of the feedback loop consisting of common gate and common drain stages. Then, a tunable ultra-wideband (UWB) bandpass filter (BPF) is designed by cascading two such inductors back-to-back through a varactor. The proposed active inductor and the BPF are designed and simulated in 90nm CMOS digital process. The inductor exhibits inductive impedance in the range from few MHz to over than 20GHz and achieves Q-factor of 600. The designed BPF shows a -3dB bandwidth of 2.25GHz with a tuning range of 5GHz.**

Index terms: active inductor, negative impedance converter, UWB band-pass filter

I. Introduction

ACTIVE inductors (AIs) are paid much attention in the design of RF and microwave circuits because of their numerous advantages over on-chip passive inductors. The advantages of AIs are large inductance values (over 10nH), high quality factors (Q >30), small chip area and tuning ability [1-2]. In CMOS processes, the series resistance of metal lines and close proximity of the substrate involving the substrate loss result in a low Q-factor of on-chip passive inductors. In addition, this proximity provides capacitive coupling between the inductor and the substrate and forces these inductors to have a low self-resonance frequency [3-4]. On the other hand, AIs can be realized with circuits consisting of a few transistors and can overcome the above limitations of on-chip passive inductors.

CMOS AIs reported in [1-2, 5-8] are based on a well-known gyrator-capacitor (gyrator-C) topology. They emulate the inductive input impedance, Z_{in}, of the two-port gyrator network loaded by capacitor. The authors in [1-2, 5-8] indicate that the input impedance of such AIs is a second order transfer function over the frequency range of interest. Two important parameters of this transfer function are the resonance frequency, ω_0, and the quality factor Q. High ω_0 ensures wide frequency range of inductive impedance where Z_{in} is an increasing function of frequency (it decreases after ω_0). High ω_0 also means high Q in applications defined by the ratio $\omega_0/\Delta\omega$. However, even with low ω_0, low frequency range and narrow tuning range, these inductors find their applications in the design of narrowband filters and amplifiers.

A wide-range tunable CMOS AI based on a cross-coupled pair of transistors providing positive feedback for enhanced Q-factor, and high ω_0 (12.5GHz) has been reported [9]. This inductor exhibits inductive impedance in the range from few MHz to the values above 10 GHz.

To widen the operating frequency range even further for new applications, the AIs that work well beyond the UWB frequency range (3.1-10.6 GHz) are required. In this paper, we propose AI also based on a cross-coupled pair of transistors. In addition, we are using a loop-gain-increasing transistor to enhance ω_0, and to increase the inductive impedance range above the upper limit of the UWB range. Using the proposed inductor, we also designed a wide-range tunable UWB band-pass filter (BPF).

The proposed AI and BPF are designed and simulated in STMicroelectronics 90nm digital CMOS process.

II. Active Inductor Design

The AI based on a cross-coupled pair of transistors forming negative impedance circuit and providing positive feedback is shown in Fig. 1 [9].

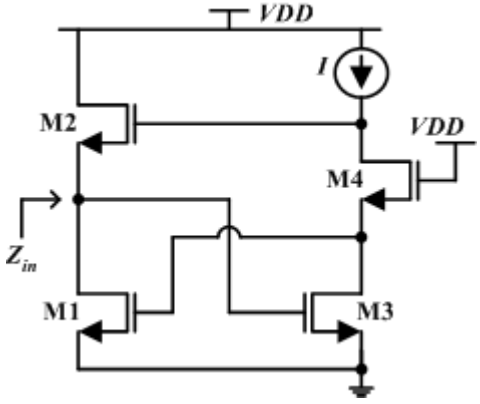

Fig. 1 AI with a cross-coupled pair of transistors

The simplified expressions for input impedance Z_{in} and its parameters ω_0 and Q at mid-frequencies are given as:

$$Z_{in} \approx \frac{\left(C_{gs2}+C_{gs4}\right)s}{C_{gs3}\left(C_{gs2}+C_{gs4}\right)s^2+C_{gs3}g_{m4}s+g_{m3}\left(g_{m4}-g_{m2}\right)} \quad (1)$$

$$\omega_0^2 \approx \frac{g_{m3}\left(g_{m4}-g_{m2}\right)}{C_{gs3}\left(C_{gs2}+C_{gs4}\right)} \quad (2)$$

$$Q \approx \frac{\omega_0\left(C_{gs2}+C_{gs4}\right)}{g_{m2}} \quad (3)$$

The stable operation of the circuit in Fig. 1 is limited with the condition that g_{m4}>g_{m2}, as expressed by (2). The subtraction of g_{m2} from g_{m4} also reduces the resonance frequency ω_0. The condition g_{m4}> g_{m2} apparently limits also the tuning range as controlled by the current I (Fig. 1).

The proposed new active inductor is shown in Fig. 2. Instead of direct cross-coupling the transistors M1 and M3, an intermediate common-source (CS) gain stage is inserted between them. The signal from the cascoded CS stage is fed to M5 and its output is connected to the gate of M1.

If each transistor is modeled by the gate-source capacitance C_{gs} and transconductance g_m, and the output conductance g_{ds} (g_m>>g_{ds}) and the gate-drain capacitance C_{gd} (C_{gs}>> C_{gd}) are neglected, then the simplified small-signal equivalent circuit of the proposed inductor (Fig. 2) may be shown as in Fig. 3.

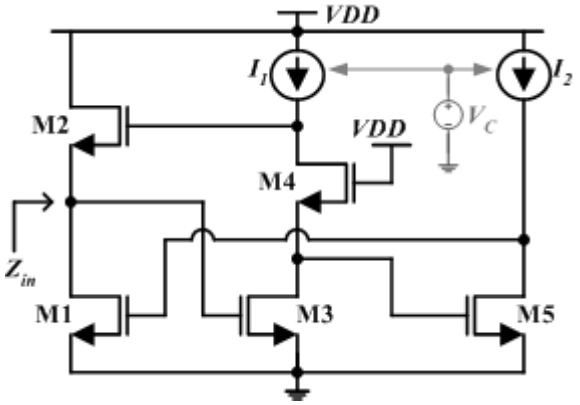

Fig. 2 The proposed new active inductor

The input admittance Y_{in} =$1/Z_{in}$ of this circuit is expressed as:

$$Y_{in}=\frac{1}{Z_{in}}=sC_{gs3}+\frac{g_{m1}g_{m3}g_{m5}}{sC_{gs1}\left\{g_{m4}+s\left(C_{gs4}+C_{gs5}\right)\right\}} + \frac{g_{m2}g_{m3}g_{m4}}{sC_{gs1}\left\{g_{m4}+s\left(C_{gs4}+C_{gs5}\right)\right\}}+\frac{g_{m3}g_{m4}}{g_{m4}+s\left(C_{gs4}+C_{gs5}\right)} \quad (4)$$

At very low frequency (*LF*) and very high frequency (*HF*), Z_{in} can be simplified as:

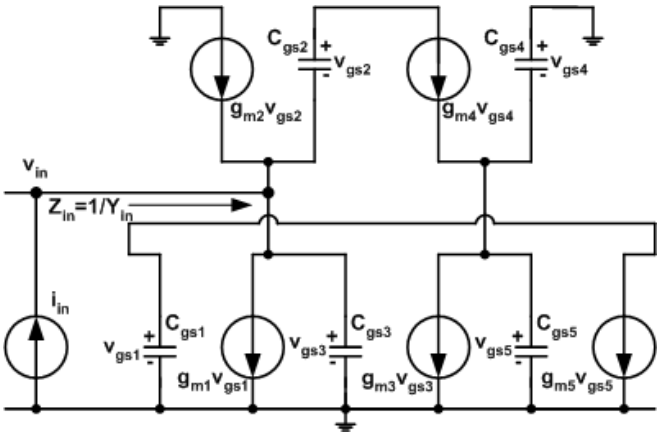

Fig. 3 The small-signal circuit of the proposed AI

$$Z_{in(LF)}=\frac{C_{gs1}C_{gs2}g_{m4}}{g_{m3}\left(g_{m1}g_{m5}C_{gs2}+g_{m2}g_{m4}C_{gs1}\right)} \quad (5)$$

$$Z_{in(HF)}=\frac{1}{sC_{gs3}} \quad (6)$$

Note that at low frequencies Z_{in} remains constant and at very high frequencies it is capacitive. At mid-frequencies, the frequency of interest over which input impedance is inductive, Z_{in} is simplified as:

$$Z_{in} \approx \frac{C_{gs1}C_{gs2}\left(C_{gs4}+C_{gs5}\right)s}{C_{gs1}C_{gs2}C_{gs3}\left(C_{gs4}+C_{gs5}\right)s^2+C_{gs1}C_{gs2}C_{gs3}g_{m4}s+C_{gs1}C_{gs2}g_{m3}g_{m4}} \quad (7)$$

The expression (7) for Z_{in} is a required second-order transfer function, which has the characteristics of a 2nd order bandpass filter. The parameters of this filter, namely ω_0 and Q, are expressed as:

$$\omega_0^2=\frac{g_{m3}g_{m4}}{C_{gs3}\left(C_{gs4}+C_{gs5}\right)} \quad (8)$$

$$Q=\frac{\omega_0\left(C_{gs4}+C_{gs5}\right)}{g_{m4}}=\frac{g_{m3}}{\omega_0 C_{gs3}} \quad (9)$$

Z_{in} peaks at ω=ω_0 and the maximum value of Z_{in} is:

$$Z_{in(\max)}=\frac{C_{gs4}+C_{gs5}}{C_{gs3}g_{m4}} \quad (10)$$

Note that ω_0 is always real as there is no subtraction term like in (8). Hence, the conditional stability problem of the active inductor shown in Fig. 1(as expressed by (2) for ω_0) has vanished. The frequency ω_0 will also be higher in the circuit of Fig. 3 as there is no subtraction term of transconductances. Overall, the increased ω_0 means increased inductive impedance range. The ω_0 and Q vary simultaneously with changing the currents I_1 and I_2 and so does $Z_{in(max)}$ given by (10). Decreasing g_{m3} or g_{m4} (which is depending on I_1), $Z_{in(max)}$ can be increased and a high value of inductive impedance can be achieved before the circuit goes into triode operation. The currents I_1 and I_2 are

controlled by a single DC voltage V_C (shown as external and shaded in Fig. 2).

III. UWB Bandpass Filter Design

To demonstrate the capabilities of the proposed active inductor, a BPF filter is designed using this circuit. Two AIs are cascaded back-to-back through a variable capacitor (varactor) C_{var} (Fig. 4). The connection results in a 4th order filter. This BPF can be tuned over the wide range of UWB frequencies (3.1-10.6GHz) using current I_1 (via V_C, see Fig. 2). C_{var} can also provide a very limited tuning.

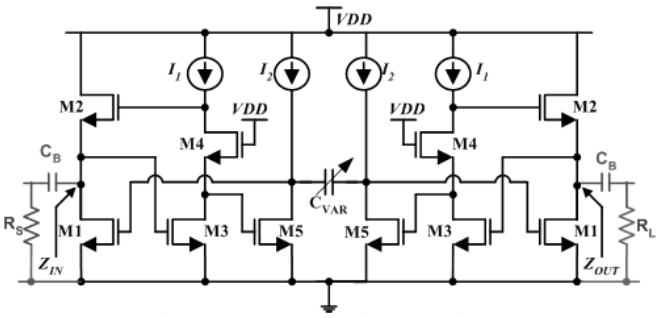

Fig. 4 UWB BPF using the proposed AI

IV. Design Realization and Simulation

The proposed AI circuit (Fig. 2) is designed and simulated in STMicroelectronics 90nm digital CMOS process using Cadence SpectreRF simulator**.** All transistors have the length (L) of 0.1µm and the widths (W) of M1, M2, M3, M4 and M5 are chosen as 3.5 µm, 5µm, 5µm, 7.5µm, 1.5µm and 2.5µm, respectively. The current sources I_1 and I_2 are realized with PMOS devices (W_{MP1}=1µm & W_{MP2}=2.5µm). The common control voltage V_C is varied from 400mV to 700mV to tune the inductor. With a power supply of 1.2V and V_c of 500mV, the proposed AI consumes 550µW.

Fig. 5 shows the AI input impedance (Z_{in}) frequency characteristics. For a control voltage of 500mV (I_1=85µA and I_2=260µA), the magnitude of Z_{in} is 237KΩ at ω_0=23.1 GHz. Note that the inductive impedance range (linear region in Fig. 5) is extended from 60MHz to over 20GHz and with positive phase angle. With the above operating condition, the calculated (via equation (10)) $Z_{in(max)}$ is 223KΩ, which is close to the simulated peak value (237KΩ). Fig. 6 shows Z_{in} for different values of control voltage V_C (varying current I_1 and I_2). A wide tuning range is achieved for the inductive impedance. Z_{in} peaks to 56KΩ at 5.5GHz for Vc of 650mV. With V_c of 450mV, Z_{in} peaks to 50KΩ at 28GHz. The variation of ω_0 and Q with V_C (I_1 and I_2) is shown in Fig. 7. Note that Q has a value of 600 which is now beyond any practical applications. The resonance frequency ω_0 is increasing with the decreasing the control voltage V_C or increasing with currents I_1 and I_2.

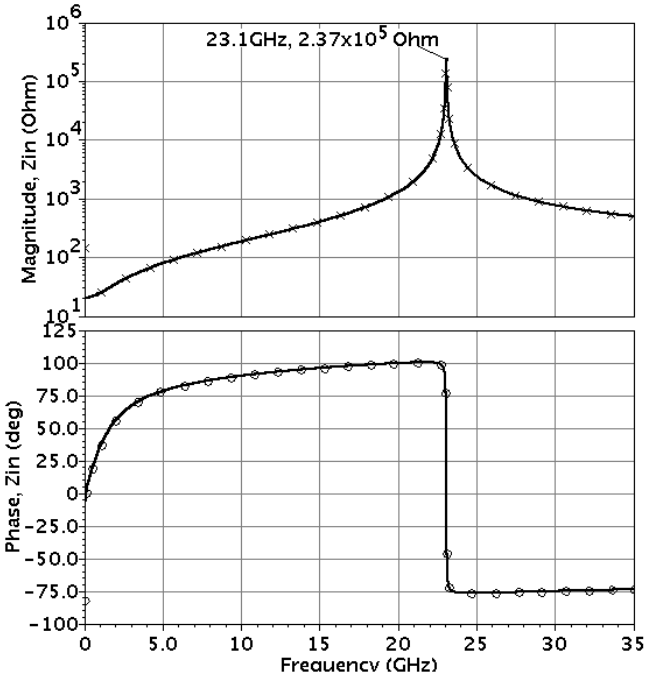

Fig. 5 Magnitude and phase of Z_{in} over frequency

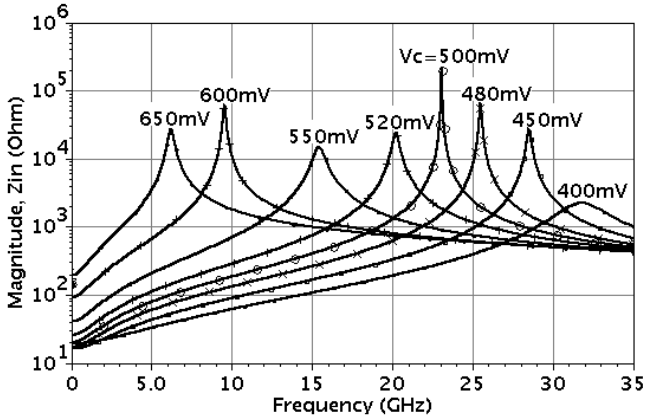

Figure 6: Z_{in} for different control voltages (V_C)

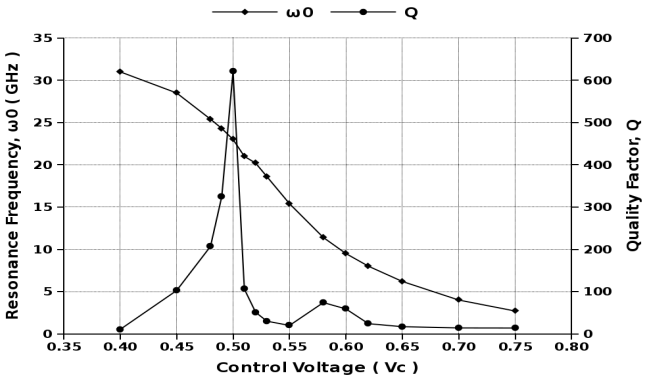

Fig. 7 ω_0 and Q over control voltage V_c

The proposed BPF is designed and simulated by scaling

up all the devices of the AI by 4 times i.e. the width of the devices in the BPF is $W_{n,BPF}$=4x $W_{n,\ AI}$, where n=1 to 5. The PMOS devices for I_1 and I_2 are also scaled up accordingly. The varactor, C_{var} is realized with two back-to-back connected PMOS devices (W/L=100 µm /0.5µm) and the control voltage is applied to these combined gates through a 100KΩ resistor (external).The frequency responses of the proposed BPF with 500Ω resistors at both ends (R_S at source and R_L at load) are shown in Fig. 8 for two different values of control voltages. With a fixed control voltage of V_{C1}=0.7V (not shown) for current I_1, the BPF shows wide tuning range for V_{C2} (not shown) controlling I_2. Note that the center frequency (f_0) of the BPF is shifted from 4.8GHz (V_{C2}=0.7V) to 8.63GHz (V_{C2}=0.5V) with a -3dB bandwidth of 2.25GHz. By varying the tuning voltage of the varactor (not shown), the bandwidth can be tuned within 200MHz only. Fig. 9 shows the wide tuning range of the UWB BPF for different values of V_{C2} with fixed V_{C1} of 700mV. Note that the centre frequency is shifted from 1.84GHz (V_{c2}=800mV) to 11.47GHz (V_{c2}=500mV). With V_{C1}=0.7V and V_{C2}=0.7V, the BPF filter shows f_o of 4.8GHz, the bandwidth of 2.28GHz and consumes a power of 1.72mW.

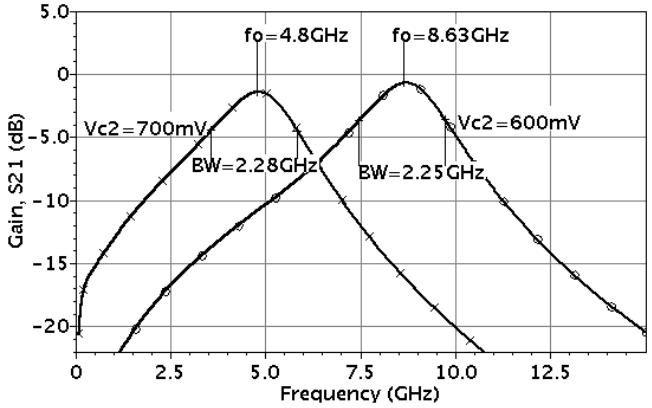

Fig. 8 Frequency response (Gain) of the UWB BPF

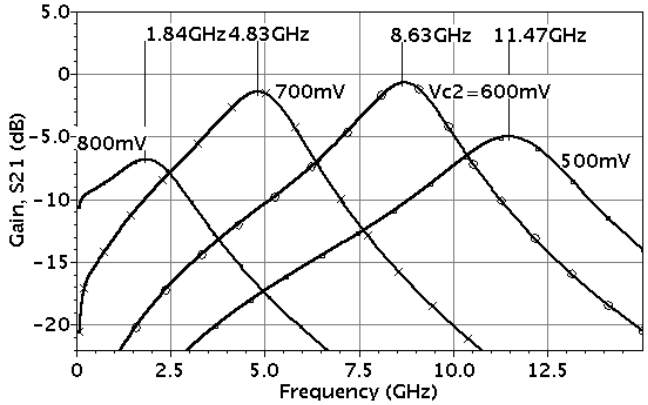

Fig. 9 Tuning of the UWB BPF with V_{C2}

V. Conclusion

A new active inductor exhibits inductive impedance in the wide frequency range (over 20GHz). This new circuit would make more flexible the design of UWB filters and amplifiers. The proposed inductor is suitable for UWB filter design with center frequency tuning range of 5GHz. Yet, the proposed active inductor exhibits very high resonance frequency (23GHz), very high Q (600) and high inductance impedance ($Z_{in(max)}$=241KΩ) value at the cost of sub-mW power (0.550mW), and the inherent noise contribution of the devices might be important. To minimize the noise contribution the circuit transistors should be kept in saturation. Our future investigation may include the noise analysis of the proposed active inductor.

The proposed filter with the bandwidth of 2.5GHz can be used in the design of multiband orthogonal-frequency-division-multiplexing (MB-OFDM) UWB transceiver. In the MB-OFDM technique, the UWB spectrum of 7.5 GHz (3.1-10.6GHz) is divided into 14 bands of 528 MHz each. Hence, the proposed UWB BPF should be able to operate at different center frequencies of different bands and band groups spreading over 3.1-10.6 GHz.

References

[1] A. Thanachayanont, and A. Payne, "VHF CMOS integrated active inductor," *Electronics Letters*, Vol. 32, No. 11, 23 May 1996, pp. 999-1000.

[2] Y. Wu, X. Ding, M. Ismail, and H. Olsson, "RF bandpass filter design based on CMOS active inductors," *IEEE Transactions on Circuits and Systems-II: Analog and Digital Signal Processing*, vol. 50, pp. 942-949, Dec. 2003.

[3] Thomas H. Lee, *The Design of CMOS Radio-Frequency Integrated Circuits*, Cambridge University Press, Cambridge, UK, 2002.

[4] John Rogers, and Calvin Plett, *Radio Frequency Integrated Circuit Design*, 2003 ARTECH House Inc., Norwood, MA, USA.

[5] Z. Gao, M. Yu, and J. Ma, "Wide tuning range of a CMOS RF bandpass filter for wireless application," *2005 IEEE Conference on Electron Devices and Solid-State Circuits*, Dec 19-21, 2005, pp. 53-56.

[6] A. Thanachayanont, "CMOS transistor-only active inductor for IF/RF applications", *Proc. IEEE International Conf. on Industry Technology (ICIT'02)*,Thailand, 2002, pp.1209-1212.

[7] K.J.P. Allidina, and S. Mirabbasi, " A widely tunable active RF filter topology," *2006 IEEE Int. Symp. on Circuits and Systems*, 21-24 May, 2006, pp. 879-882.

[8] S. Sae-Ngow, and A. Thanachayanont, "A low-voltage, wide dynamic range CMOS floating active inductor," *TENCON 2003 Conference on Convergent Technologies for Asia-Pacific Region*, vol.4, no., pp. 1460-1463 Vol.4, 15-17 Oct. 2003.

[9] M.M. Reja, I.M. Filanovsky , and K. Moez , "Wide Tunable CMOS Active Inductor," *IEE Electronics Letters*, pp. 1461-1463, Dec. 2008